

## CORRELATION STUDIES OF THE LOW-ENERGY ${}^6\text{Be}$ SPECTRUM

V. CHUDOBA<sup>1,2</sup>, A. S. FOMICHEV<sup>1</sup>, I. E. EGOROVA<sup>3</sup>, S. N. ERSHOV<sup>3</sup>,  
M. S. GOLOVKOV<sup>1</sup>, A. V. GORSHKOV<sup>1</sup>, V. A. GORSHKOV<sup>1</sup>,  
L. V. GRIGORENKO<sup>1</sup>, G. KAMIŃSKI<sup>1</sup>, S. A. KRUPKO<sup>1</sup>, I. G. MUKHA<sup>3</sup>,  
YU. L. PARFENOVA<sup>1</sup>, S. I. SIDORCHUK<sup>1</sup>, R. S. SLEPNEV<sup>1</sup>, L. STANDY LO<sup>1</sup>,  
S. V. STEPANTSOV<sup>1</sup>, G. M. TER-AKOPIAN<sup>1</sup>, R. WOLSKI<sup>1</sup>, M. G. ZHUKOV<sup>4</sup>

<sup>1</sup>*FLNR, JINR, Dubna, 141980, Russia*

<sup>2</sup>*Institute of Physics, Silesian University in Opava, Opava, Czech Republic*

<sup>3</sup>*BLTP, JINR, Dubna, 141980, Russia*

<sup>4</sup>*Fundamental Physics, Chalmers University of Technology, Göteborg, Sweden*

By using the  ${}^1\text{H}({}^6\text{Li}, {}^6\text{Be})n$  charge-exchange reaction, population of continuum states in  ${}^6\text{Be}$  was observed up to 16 MeV above its three-body decay threshold. In kinematically complete measurements performed by detecting  $\alpha+p+p$  coincidences the spectrum provides detailed correlation information about the  $0^+$  ground state and first excited  $2^+$  state. Influence of reaction mechanism on formation of observed spectra is discussed.

### 1. Introduction

Structure of  ${}^6\text{Be}$  has been repeatedly investigated both theoretically and experimentally [1–6]. This nucleus is interesting because of two aspects: it is the lightest possible two-proton emitter and it is the mirror isotope to  ${}^6\text{He}$  [6]. Generally, three circumstances form results when one investigate the unbound nuclei: final state interaction (FSI) of all products, reaction mechanism and

initial system. When we are dealing with long living resonances, FSI overshadow the latter two factors, because system lives enough long to lose information about its creation. However, all three aspects should be taken into account to properly elucidate obtained data when dealing with broad, short living resonances.

Our work is mainly aimed to the interpretation of the  $\alpha+p+p$  continuum spectrum and its decomposition to particular states. Except for known states  $0^+$  at  $E_T = 1.37$  MeV and  $2^+$  at  $E_T = 3.05$  MeV ( $E_T$  is three-body decay energy), spectrum is formed by  $J^-$  states at energies above the  $2^+$  state [7]. This study is rather qualitative and searches for the most important aspects which affect the spectrum formation.

The  ${}^6\text{Be}$  spectrum was populated in the charge-exchange  $p({}^6\text{Li}, {}^6\text{Be})n$  reaction. This reaction was chosen because of its presumably simple mechanism. Another reason for this choice was that, due to the inverse kinematical character of this reaction, the  ${}^6\text{Be}$  decay products ( $\alpha+p+p$ ) fly out in relatively narrow cone in the forward direction in laboratory frame. The latter allows us to detect all decay products with reasonable efficiency in a wide range of  $E_T$ . More detailed information about experiment can be found in Ref.[7].

## 2. Theoretical model

We consider the model which includes only the population of  $0^+$  and  $2^+$  states in this work. In total, there are eight degrees of freedom for investigated process. We have chosen the four related to nuclear structure and four to reaction mechanism. Four of them describes internal correlations of  ${}^6\text{Be}$  nucleus:  $E_T$ , energy distribution parameter  $\varepsilon = E_{pp}/E_T$  ( $E_{pp}$  is kinetic energy of relative motion of two protons) and two angles between Jacobi momenta. The center of mass (CMS1) of  $p({}^6\text{Li}, {}^6\text{Be})n$  reaction orientation can be described by angles  $(\theta_r, \varphi_r)$  and  ${}^6\text{Be}$  orientation center of mass system relative to the direction of transferred momentum (CMS2) is described by  $\rho$ -matrix.

Generally, two states with different  $J^\Pi$  can interfere. Effect of interference of the  $0^+$  and  $2^+$  states to the population cross section can be expressed as

$\sigma \sim |A_{0^+} + e^{i\phi_{02}} A_{2^+}|^2$  where  $\phi_{02}$  is relative phase between transition amplitudes  $A_{0^+}$  and  $A_{2^+}$ . Theoretical model describing three-body  $\alpha+p+p$  FSI is described in Refs. [6,7].

### 3. Data analysis

Invariant mass  ${}^6\text{Be}$  spectrum obtained from triple  $\alpha+p+p$  coincidences in the whole angular range of the  ${}^1\text{H}({}^6\text{Li}, {}^6\text{Be})n$  reaction is presented in Fig. 1(a).

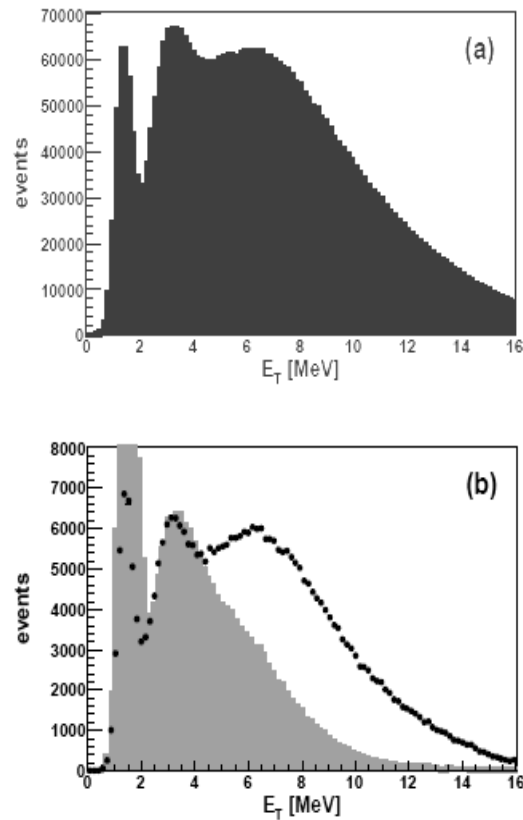


Fig. 1. Invariant mass spectrum (a) complete experimental data; (b) cut of  $\theta_r \rightarrow (40 \div 50)^\circ$ , dots represent experimental data, gray histogram MC simulations

Two prominent peaks related to the population of the ground  $0^+$  and first excited  $2^+$  states are superimposed on the broad continuum. The width of the

peak corresponding to the population of the ground state demonstrates overall instrumental resolution. Registration of the triple co- incidences corresponds to complete kinematics measurement and we can consider the population and the decay of  ${}^6\text{Be}$  system in detail. We will focus our attention on the parameters of the model related to the reaction mechanism and how they affect on the formation of the measured spectra. We have restricted our analysis by consideration of  $\theta_r \rightarrow (40, 50)^\circ$ . This region has been chosen because all components of the spectrum ( $0^+$ ,  $2^+$  states and continuum) are well pronounced there. Such a narrow angular range allows us to neglect angular dependence of the population amplitudes for different states and consider their ratio as the model parameter. As a first iteration the ratio of population probabilities can be found from comparison of the calculations with experimental spectrum at the energies of corresponding maxima.

The experimental spectrum together with model calculations for  $\theta_r \rightarrow (40\div 50)^\circ$  are presented in Fig. 1(b). The model calculations include correction for efficiency of registration made by Monte Carlo method to take into account all details of the experimental setup. The result of the calculation is normalized for maximum of first excited state. Deficit of the model prediction for high energy part of the spectrum is present in Fig. 1(b) on account of our simplified model. Since we consider the energy region  $E_T < 1.37$  MeV, there are no free model parameters related to the reaction mechanism. The angular distributions of the decay products from only  $J^\pi = 0$  should be uniform in the CMS 2. Distributions of all variables exhibit good agreement between calculations and experimental data in this energy region. Besides the validity of the theoretical model, obtained agreement demonstrates correctness of registration efficiency. If few states may contribute to the formation of the spectrum, the nature of the all distributions becomes more complicated.

Comparison of  $\varepsilon$  distribution measured for  $E_T \rightarrow (2\div 3)$  MeV with results of four theoretical calculations with different sets of model parameters is presented in Fig. 2. Dots with error bars show the measured distribution of the  $\varepsilon$ , the gray histogram shows the MC simulated data where model calculations were taken as an input.

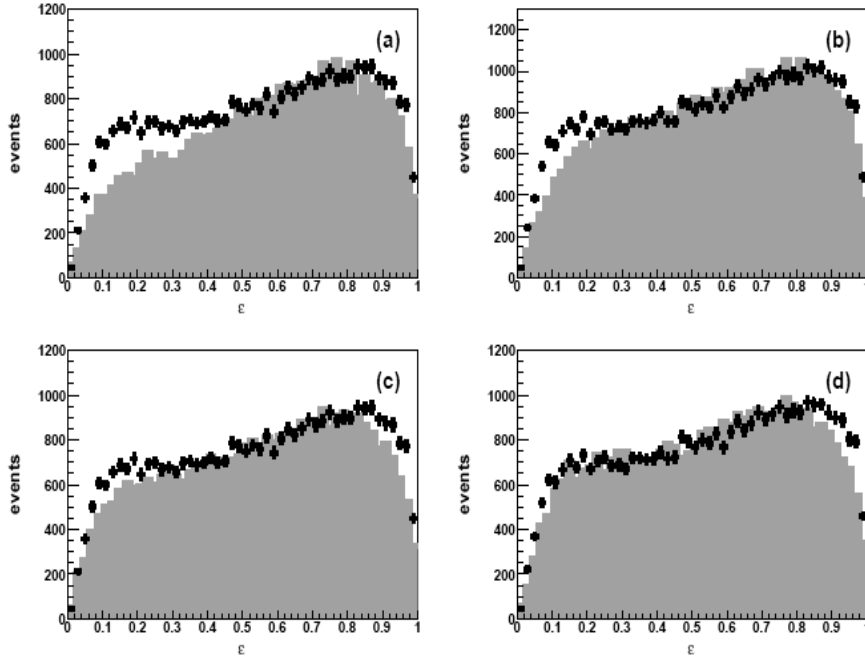


Fig. 2. Parameter of energy distribution  $\varepsilon$  for  $E_T \rightarrow (2\div 3)$  MeV, dots with error bars represents experimental data, gray histogram MC simulations with different model parameters: (a)  $\varphi_{02} = \Pi$ , full alignment; (b)  $\varphi_{02} = 0$ , full alignment; (c)  $\varphi_{02} = \Pi$ , no alignment; (d)  $\varphi_{02} = 0$ , no alignment

The ratio of population probability of ground and first excited states was taken the same for all variants and only parameters governed by the reaction mechanism were varied. Upper row corresponds to the complete spin alignment of the first excited state ( $J^\Pi = 2^+$  has only zero projection on the axis of transferred momentum). Bottom row corresponds to the case of equal population probabilities of all possible spin projections. The value of  $\varphi_{02}$  was taken equal to  $\Pi(0)$  radians was for the left (right) column. Four panels of Fig. 2 demonstrate strong dependence of MC simulations on the parameters related to the reaction mechanism. Initial distributions over  $\varepsilon$  (undisturbed by the registration efficiency) are the same for all variants. It results in severe problems to get precise information about properties of the studied system,

because we have to take into account all features of the reaction which lead to population of the spectrum. We have considered distributions of variables directly related to the system orientation to better distinguish the effects of reaction mechanism and internal structure of decaying system. Angular distributions of the protons in the CMS 2 are shown in Fig. 3. Four panels of the figure correspond to the same model assumptions as in Fig. 2. We treat spectra in quasi-binary approximation ( $\epsilon > 0.8$ ) to emphasize the specific features of angular distributions with definite angular momentum.

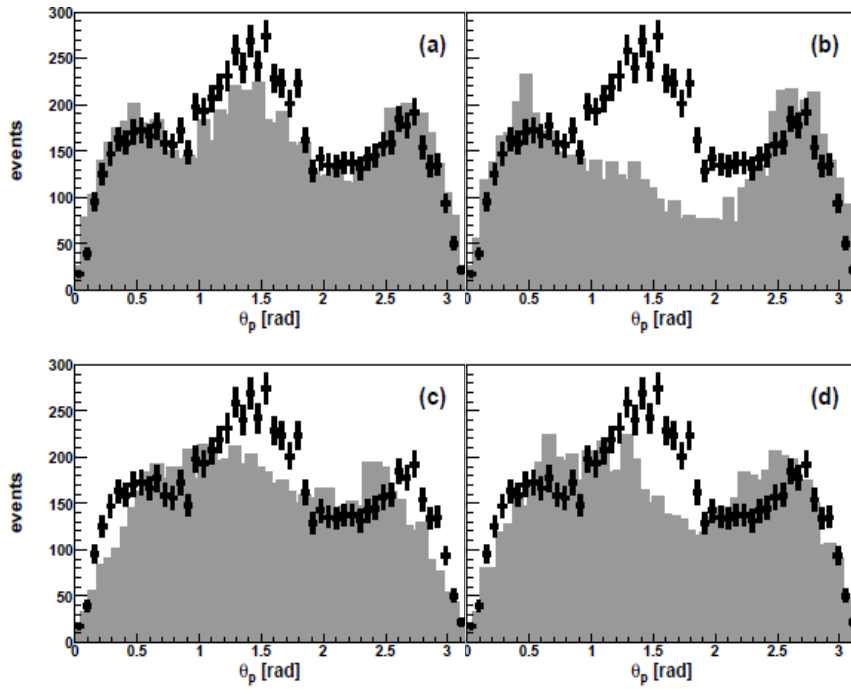


Fig. 3. Angle  $\theta_p$  of proton in respect to the axis of transferred momentum, dots with error bars represents experimental data, gray histogram MC simulations with different model parameters: (a)  $\varphi_{02} = \Pi$ , full alignment; (b)  $\varphi_{02} = 0$ , full alignment; (c)  $\varphi_{02} = \Pi$ , no alignment; (d)  $\varphi_{02} = 0$ , no alignment

One can see dramatic changes for MC simulations obtained with different model parameters. The case of complete alignment with  $\varphi_{02} = \Pi$  (Fig. 3(a)) remains the experimental data more then other panels. It looks like the

experimental data can be easily fitted by small variation of the model parameters. Complete alignment of the  ${}^6\text{Be}$  spin can be naturally understood if one supposes the direct character of the  ${}^1\text{H}({}^6\text{Li}, {}^6\text{Be})\text{n}$  reaction when charge-exchange is accompanied by the spin flip of interacting nucleons.

#### 4. Conclusion

${}^6\text{Be}$  was populated with sufficient efficiency in the excitation energy range up to 16 MeV and full angular range in the c.m.s. of the  ${}^1\text{H}({}^6\text{Li}, {}^6\text{Be})\text{n}$  charge-exchange reaction. The invariant spectrum shows two peaks corresponding to population of the ground  $0^+$  and the first excited  $2^+$  states. These peaks are superimposed on the broad bump with maximum at  $E_T \sim 6$  MeV. The main attention of our work was paid to the influence of reaction mechanism on spectra formation.

Model calculations are in well agreement with experimental data in the low-energy part of the spectrum (dominated by the  $0^+$  state). This observation provides evidence of validity of the applied model and correctness of registration efficiency. Analysis of the energy region  $E_T \rightarrow (2\div 3)$  MeV shows that the formation of the observed spectra strongly depends on the model parameters related to the reaction mechanism such as spin alignment and relative phase of transition amplitudes  $\varphi_{02}$ .

Comparison of the experimental proton angular distribution for  $E_T \rightarrow (2\div 3)$  MeV with the results of the model calculations provides the evidence of direct reaction mechanism. Analysis of different parameters related to reaction mechanism indicates that the value  $\varphi_{02}$  should be close to  $\Pi$ .

Complete kinematics measurements with high statistics presents a proper tool to analyze complicated spectra formed by the broad overlapping resonances. We have suggested an adequate approach to analysis of correlation experiments and we assume that obtained results have important implementations for the studies of the few-body decays in general. We expect that further correlation analysis will shed light on the structure of low energy  ${}^6\text{Be}$  spectrum.

**References**

1. D.R. Tilley et al., *Nucl. Phys.* **A708**, 3 (2002).
2. X. Yang et al., *Phys. Rev.* **C52**, 2535 (1995).
3. V. Guimarães et al., *Nucl. Phys.* **A722**, 341c (2003).
4. P. Papka et al., *Phys. Rev.* **C81**, 054308 (2010).
5. L.V. Grigorenko et al., *Phys. Lett.* **B677**, 30 (2009).
6. L.V. Grigorenko et al., *Phys. Rev.* **C80**, 034602 (2009).
7. A. S. Fomichev et al., *Phys. Lett.* **B708**, 6 (2012).